ELSEVIER

Journal of Chromatography A, 944 (2002) 93–117

JOURNAL OF CHROMATOGRAPHY A

www.elsevier.com/locate/chroma

Optimal design of batch and simulated moving bed chromatographic separation processes

Andreas Jupke, Achim Epping, Henner Schmidt-Traub*

Chair of Plant Design, Department of Chemical Engineering, University of Dortmund, D-44221 Dortmund, Germany

Abstract

Preparative chromatography, especially simulated moving bed (SMB) chromatography, is a key technology for the separation of fine chemicals on a production scale. Most of the design methods for batch and SMB processes proposed in the open literature deal with the optimisation of the operating conditions for a given chromatographic unit only. Therefore, a comparison of the process economy may lead to incorrect results. In this contribution, an effective strategy for the optimal choice of all process parameters (operation and design parameters) is proposed. The main idea of this strategy is to apply a detailed and experimentally validated process model and to reduce the number of influencing parameters by introducing and optimising dimensionless process parameters. It is shown that there is an infinite choice of design and operating parameters to achieve maximum productivity or minimum separation costs and not at the maximum pressure drop only. The detailed design of the chromatographic unit and the selection of the operating conditions can be adjusted by considering the availability of columns and packing materials. As the model system, the separation of a racemic mixture (EMD53986) on Chiralpak AD was investigated. After complete optimisation of a batch and a SMB unit, a real comparison of the process economy can be achieved. Finally, the influences of two different objective functions, productivity and specific separation cost, are analysed. © 2002 Elsevier Science B.V. All rights reserved.

Keywords: Preparative chromatography; Simulated moving bed chromatography; Enantiomer separation; Optimization; Computer simulation; EMD53986

1. Introduction

In the pharmaceutical and fine chemical industry, complex mixtures of similar substances, in particular enantiomers, are often obtained. Accordingly, chromatographic separations are attracting increasing interest for the purification of these products. This trend is also supported by the expanding demand for optically pure compounds and the restricted use of racemic drugs. The parameters influencing chromatographic batch processes and their effect on process performance are discussed and summarised in Refs. [1,2].

Employment of the continuous simulated moving bed (SMB) process in large-scale applications has a proven ability to reduce separation costs. The SMB process was developed in the early 1960s by Broughton and Gerhold [3] and has been used for many years in the petrochemical and sugar industries for large-scale separation [4,5]. Recently, the separation of enantiomers due to the demand for high-purity products has become necessary [34]. These applications have been reviewed by Ditz et al. [6].

Fig. 1 shows the working principle and the internal concentration profile of the SMB process. A

*Corresponding author. Tel.: +49-231-755-2338; fax: +49-231-755-2341.

E-mail address: schmtr@ct.uni-dortmund.de (H. Schmidt-Traub).

0021-9673/02/$ – see front matter © 2002 Elsevier Science B.V. All rights reserved.
PII: S0021-9673(01)01311-5

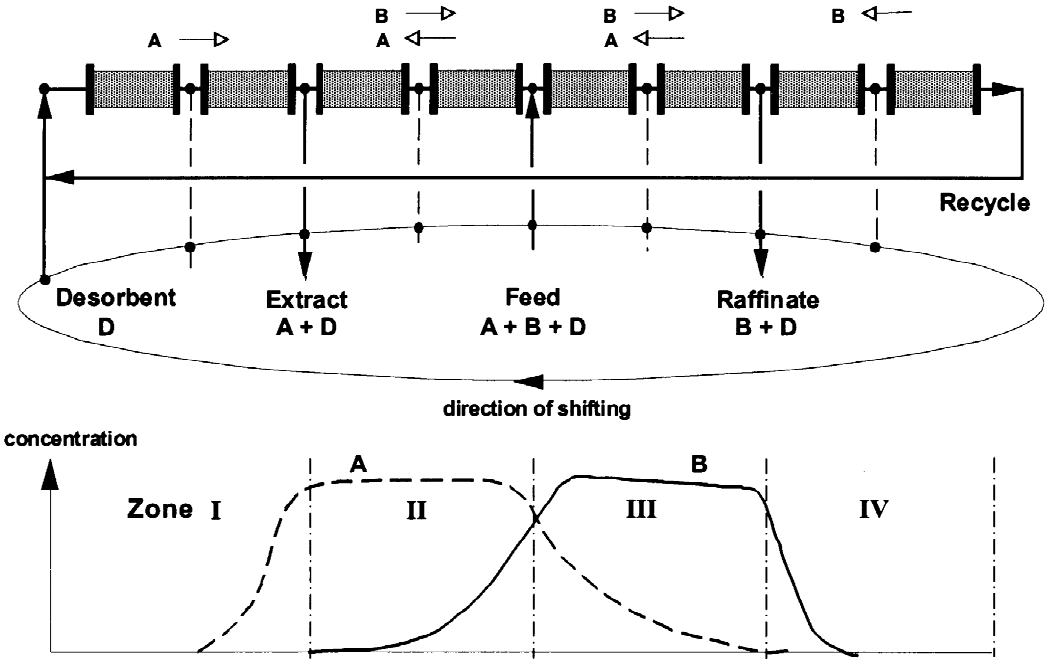

Fig. 1. Operating principle and internal concentration profile of the simulated moving bed (SMB) process.

SMB unit consists of several (six to 24) columns connected in series. The SMB technique is based on the simulated countercurrent flow between the mobile phase and the stationary phase. This countercurrent movement is achieved by sequentially shifting the inlet and outlet ports in the direction of the liquid flow.

A feed, consisting of a binary mixture to be separated, is introduced into the plant. The less-adsorbed component B is carried with the liquid flow and can be collected in the raffinate. The more-adsorbed component A migrates in the direction of the simulated solid flow and is drawn off in the extract. In order to achieve complete separation of the feed components, the internal flow-rates of the liquid phase within each zone as well as the shifting time corresponding to the simulated solid flow have to be determined.

In general, there are two factors that impede the development of optimisation strategies for chromatographic processes which cover the whole range of available optimisation parameters. First, there is the complex dynamic behaviour of overload chromatographic separations, especially for continuous processes. Second, there is the large number of parameters which influence the performance and the economy of the process.

In recent decades, much effort has been expended on the development of optimisation strategies for chromatographic separations. Several groups have proposed approaches which differ in the type of process model and the objective functions. First, we will give a brief summary of the important approaches for batch and SMB separation and point out the advantages and disadvantages. Subsequently, a new complete optimisation approach will be presented. Furthermore, the results and advantages of this new approach will be discussed.

1.1. Batch chromatography

The degrees of freedom to optimise the design of a batch separation are the flow-rate, column length, injection time, and the cut times for fraction collection. The column diameter is generally assumed to be a scale parameter. For batch chromatography, two fundamentally different cut and fraction collection strategies for an optimal separation of a binary mixture can be distinguished. Both approaches are shown in Fig. 2.

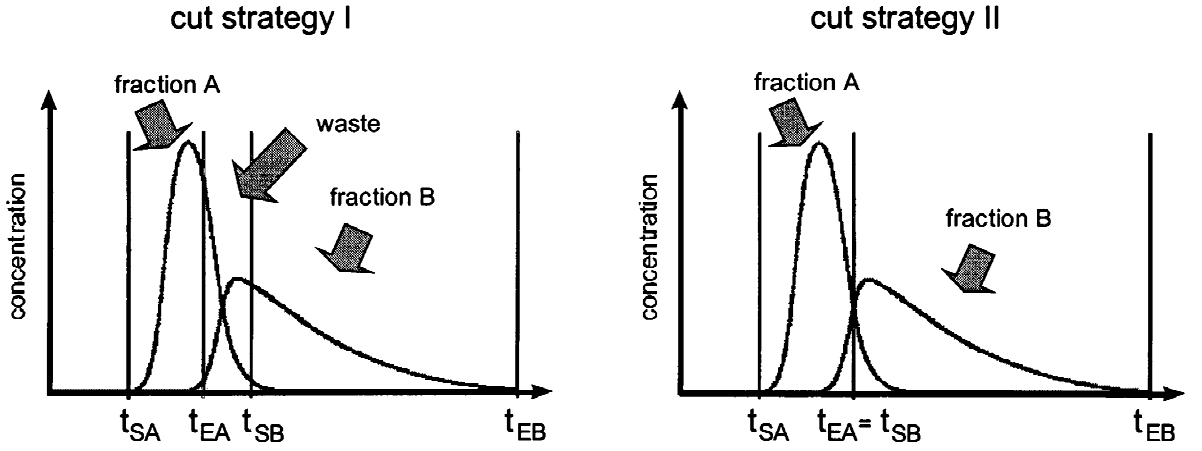

Fig. 2. Cut strategies for batch optimisation: (I) three fractions, (II) two fractions.

Felinger and Guiochon [2,7–9] applied cut strategy I in Fig. 2. One fraction for each compound A and B and a waste fraction are collected. Therefore, four cut times have to be adjusted. The collection of compound A starts at time t_{SA} and ends at t_{EA}. Then a waste fraction elutes until the collection of compound B starts at t_{SB} and ends at t_{EB}. To describe the separation process, an equilibrium dispersive model [10] with an apparent dispersion coefficient was used.

In contrast to that approach, the methods of Strube et al. and Dünnebier are based on the use of more sophisticated process models such as a lumped kinetic model [11] and a general rate model [13], respectively. The second, more important difference is the application of cut strategy II of Fig. 2. Here, two fractions are collected only. Fig. 2 illustrates that, for strategy II, the cut time for the end of fraction A, t_{AE}, is the starting time for the collection of fraction B, t_{SB}. When high purity is demanded, which is usually the case in pharmaceutical and fine chemical applications, cut strategy II further requires almost baseline separation between the two injected compounds. In this contribution it will be shown that cut strategy II leads to a significant decrease in the specific productivity and an increase in specific eluent consumption in comparison to cut strategy I. Consequently, strategy II will not lead to an economically optimal separation process with minimum separation costs.

The contributions of Felinger and Guiochon [2,7–9] differ in the use of the objective function. They mostly applied the productivity as the objective function [7]. In Ref. [8] the importance of the contribution of the eluent and fixed costs to the total separation costs is discussed. Therefore, Felinger and Guiochon introduced a hybrid function which considers the production rate, the specific solvent consumption and the fixed costs. However, the yield is not included in this hybrid function. For that reason, an important contribution to the total separation costs is ignored, especially in the case of high feed costs. This drawback was partially compensated by the introduction of the product yield and production rate [9]. This method was used for an extensive study of the different modes of chromatography [2]. However, by applying this function it is not possible to distinguish between high and low feed costs and, additionally, the solvent costs and the fixed costs are neglected.

1.2. SMB chromatography

Due to the complexity of the SMB process and the non-linear behaviour that it exhibits, especially under overload conditions related to non-linear and coupled adsorption isotherms, an empirical design is nearly impossible. Therefore, different types of process models are applied for the determination of the proper operating conditions. Most of the methods for the design of SMB units proposed in the open literature deal with the optimisation of the operation

conditions for a given chromatographic unit only. Therefore, comparisons of the process performance and economy between batch and SMB separation often lead to incorrect results.

Focusing on the operating parameters, a SMB unit exhibits five degrees of freedom. These are the flow-rates within the four zones as well as the switching time. The applied SMB models are mainly based on equilibrium theory, which means neglecting axial dispersion and mass transfer resistance and approximation of the SMB process by a true moving bed (TMB) system [4,14–16]. The TMB process is the exact boundary case for a SMB process with an infinite number of columns and an infinitely small switching time as well as column length.

In order to optimise the productivity, Storti et al. [14] proposed a definition for the flow-rate ratios, m_j, in the four zones:

$$m_j = \frac{\dot{Q}_j t^* - V\varepsilon_t}{V(1-\varepsilon_t)} \quad (1)$$

These ratios have to be adjusted by considering the adsorption isotherms only. Analytical solutions of this simplified model for several types of adsorption isotherm have been reported [12] and allow a fast and easy adjustment of the flow-rate ratios. The ratios of zones 2 and 3 are usually visualised in the so-called operating diagram [14].

However, by using more detailed models it can be shown that this simplified approach does not lead to the real optimum operating conditions [17,18]. Consequently, TMB models and models applying equilibrium theory are suitable for an estimate of the operating parameters only. In addition, models applying equilibrium theory do not consider the finite efficiency of chromatographic columns. Thus, an optimisation of design parameters such as column length or columns per zone is not achievable employing equilibrium theory. Detailed models are necessary. A new algorithm for the automated determination of the optimum operating conditions considering a detailed SMB model including real switching of the inlet and outlet ports was presented recently [18,19].

Only a few publications, Charton and Nicoud [32], Biressi et al. [30] and Ludemann-Hombourger et al. [35], consider the influence of the column length and particle diameter on the optimisation of the design of SMB units.

Charton et al. demonstrated that a design optimisation generally leads to low numbers of theoretical stages [32]. However, the process models usually applied for the design of chromatographic units such as the equilibrium stage model [30,32,35] and the equilibrium dispersive model [2] have the characteristic of decreasing accuracy with low number of stages [10]. This decrease in accuracy is additionally increased by applying TMB models.

Further, Charton and Nicoud, Biressi et al. as well as Ludemann-Hombourger et al. assumed that the maximum productivity will be obtained at the maximum pressure drop only. Thus, they fixed the flow-rate in zone I at its maximum. In this contribution, we demonstrate that this assumption does not hold.

1.3. Separation costs

All approaches for the design of SMB units have one factor in common, to maximise the productivity or the production rate. Economic aspects are not considered. In the literature, a few contributions discuss the cost structure of chromatographic separations as a function of the required production rate only. Usually, the product stream per volume of stationary phase is taken into account as the objective function. The triangle theory, in fact, is limited to the use of the productivity as the objective function.

Economic aspects are presented for a SMB application by Pynnonen [33], but the units are not completely optimised and a design strategy to minimise these costs is not proposed.

Strube et al. [11] compared the separation costs of SMB and batch separations for different production rates for optimised processes by using the productivity as the objective function. A summary of the results shows that the most important contribution to the total separation costs is the cost of the mobile phase with increasing production rate. In the work of Kati and Jagland [20], a complete description of the contribution of different kinds of costs to the total separation costs for batch separation is given. Also, the influence of the different physical properties of the separation system and the plant design is discussed. It is demonstrated that the cost structure of the separation problem changes with the scale of the separation. For smaller production amounts the contribution of capital, labour and maintenance costs to

the total costs is significantly higher than for a larger production rate. Similar to the results of Strube et al. [11] it was found that eluent consumption contributes significantly to the total cost of the separation. However, the applied optimisation strategy, and the approach of Strube et al., did not use the costs as the objective function. Thus, all these contributions suffer from the fact that the total separation costs and the cost structure of the separation problem were not included in the optimisation strategy.

Therefore, this contribution focuses on four aims. First, we want to show that it is necessary for batch and SMB separations to optimise the operating and design parameters simultaneously to achieve an optimal process. The second and most important point is the development of strategies for an optimal design of both processes. We will demonstrate that similar strategies for batch and SMB optimisation can be applied. Third, we demonstrate that the use of the separation costs only leads to an economically optimal process for both batch and SMB chromatography. We point out that optimising the operating conditions or choosing the wrong objective function will lead to a less economical process for batch and SMB chromatography. Finally, the separation costs of completely optimised processes are compared and the similarities of the processes are analysed.

2. Theory

2.1. Process model

The model for a chromatographic column results from differential mass balances of the liquid (Eq. (2)) and the solid phase (Eq. (3)). It takes into account convection and the important effects of nonidealities, which are axial dispersion and mass transfer between the extra- and inter-particle mobile phase as well as competitive adsorption isotherms (Eq. (4)) [18,21–23]:

$$\text{liquid phase:}\quad \frac{\mathrm{d}c_i}{\mathrm{d}t} = D_{\mathrm{ax}} \cdot \frac{\mathrm{d}^2 c_i}{\mathrm{d}x^2} - u_{\mathrm{int}} \cdot \frac{\mathrm{d}c_i}{\mathrm{d}x} - k_{\mathrm{eff},i} \cdot \frac{6}{d_{\mathrm{p}}} \cdot \frac{1-\varepsilon}{\varepsilon} \cdot (c_i - c_{\mathrm{p},i}) \qquad (2)$$

$$\text{solid phase:}\quad (1-\varepsilon_{\mathrm{p}}) \cdot \frac{\mathrm{d}y_i}{\mathrm{d}t} + \varepsilon_{\mathrm{p}} \cdot \frac{\mathrm{d}c_{\mathrm{p},i}}{\mathrm{d}t} = k_{\mathrm{eff},i} \cdot \frac{6}{d_{\mathrm{p}}} \cdot (c_i - c_{\mathrm{p},i}) \qquad (3)$$

$$\text{adsorption isotherms:}\quad y_i = f(\vec{c}_{\mathrm{p},i}) \qquad (4)$$

The dynamic model of the SMB process is obtained by connecting the models for single columns while considering the real cyclic switching of the inlet and outlet ports (node model). The resulting system of coupled partial differential equations is reduced to a system of ordinary differential equations (ODEs) using the Galerkin-Finite-Element method for the liquid phase [24]. This system of ODEs was implemented and solved within the simulation environment gPROMS (Process Systems Enterprises, London, UK). Due to this efficient numerical solution and implementation in gPROMS the computation time is about 5 min to reach the cyclic steady state for the SMB simulation of an enantioseparation on an ordinary personal computer (Pentium II, 450 MHz).

Nevertheless, it is tedious to carry out a large number of simulation studies and vary the column length, flow-rate and injection time for batch and zone flow-rates, and switching times and column length for SMB separations. Therefore, it is first necessary to reduce the number of influencing parameters to decrease the number of required simulations.

This is realised by introducing dimensionless variables for the time Θ, concentration $C_{0,i}$ and space Z, as well as the Peclet number (Eq. (6)) and modified Stanton number (Eq. (5)). Thus, the model can be rewritten in a dimensionless form (Eq. (7)):

$$St_{\mathrm{eff},i} = k_{\mathrm{eff},i} \cdot \frac{6}{\mathrm{d}_{\mathrm{p}}} \cdot \frac{L_{\mathrm{C}}}{u_{\mathrm{int}}} \qquad (5)$$

$$Pe = \frac{u_{\mathrm{int}} L_{\mathrm{C}}}{D_{\mathrm{ax}}} \qquad (6)$$

$$\frac{\mathrm{d}C_{0,i}}{\mathrm{d}\Theta} = \frac{1}{Pe} \cdot \frac{\mathrm{d}^2 C_{0,i}}{\mathrm{d}Z^2} - \frac{\mathrm{d}C_{0,i}}{\mathrm{d}Z} - St_{\mathrm{eff},i} \cdot \frac{1-\varepsilon}{\varepsilon} \cdot (C_{0,i} - C_{\mathrm{p}0,i}) \qquad (7)$$

Guiochon et al. [10] showed that, in the case of linear chromatography, the contributions of axial dispersion and mass transfer resistance are additive

and the resulting number of plates of the column can be calculated using:

$$\frac{L_C}{N_i} = \frac{2D_{ax}}{u_{int}} + 2 \cdot \left(\frac{k_i'}{1 + k_i'} \right)^2 \cdot \frac{u_{int}}{k_i' k_m} \quad (8)$$

According to Glueckauf [25] the lumped mass transfer coefficient k_m can be correlated directly, in the case of linear chromatography, with the film mass transfer coefficient k_{film} and the pore diffusion coefficient D_{pore} (Eq. (9)). In this case, the value of k_m is proportional to the ratio of the effective mass transport coefficient to the particle diameter $k_{eff,i}/d_p$ in Eq. (2):

$$k_{01} \cdot \frac{d_p}{k_{eff,i}} = \frac{1}{k_i' k_{m,i}} = \frac{d_p}{6Fk_{film,i}} + \frac{d_p^2}{60FD_{pore,i}} \quad (9)$$

Applying Eq. (9), Eq. (8) can be transformed into:

$$\frac{1}{N_i} = \frac{2D_{ax}}{u_{int} L_C} + 2 \cdot \left(\frac{k_i'}{1 + k_i'} \right)^2 \cdot \frac{k_{01} d_p}{k_{eff,i}} \cdot \frac{u_{int}}{L_C} = \frac{2}{Pe} + \frac{k_{0,i}}{St_{eff,i}} \quad (10)$$

From Eq. (7) it becomes clear that band broadening is influenced by the Peclet and Stanton numbers only. Additionally, Eq. (10) shows that the number of plates in the system is also influenced by these dimensionless numbers only.

The number of plates strictly has no physical meaning if it is determined directly from a chromatogram in the non-linear adsorption range. But the number of plates is a clear and, in practice, widespread expression of the column efficiency in linear chromatography. For higher fluid velocities it summarises the band broadening effects of dispersion and the mass transfer limitation. Both of these effects depend on the velocity. Since non-thermodynamic band broadening in non-linear chromatography is caused by the same mechanism, the number of plates determined in linear chromatography can also characterise the non-thermodynamic band broadening in non-linear chromatography.

The dependence on the fluid velocity of the experimentally determined plate heights can generally be fitted to the Van Deemter correlation (Eq. (11)) [26]. Since molecular diffusion is negligible in preparative chromatography due to the high fluid velocity, the Van Deemter correlation can be simplified:

$$HETP_i = \frac{L_C}{N_i} = A_i + B_i u_{int} + \frac{C}{u_{int}} \approx A_i + B_i u_{int} \quad (11)$$

Since the use of plate numbers to characterise the column efficiency is widely accepted in practice, we apply this characteristic parameter to summarise the influence of column length, interstitial velocity, dispersion and mass transfer. This significantly reduces the number of simulations which have to be carried out to optimise chromatographic processes.

2.2. Process performance and objective functions

A further aspect when optimising chromatographic separation processes is the choice of the objective function. There are several possible objective functions proposed in the literature. Katti and Jagland [20] have shown that different cost structures of a separation problem cause different optimal design and operating conditions.

In this contribution, the influence of two different objective functions on the design parameters of batch and SMB processes is analysed. The first type of objective function is the process performance parameters such as specific productivity, defined as the mass of product per time and volume of stationary phase, and the specific eluent consumption, defined as the volume of eluent per mass of product. The second type is the specific separation costs.

Due to the different operating parameters of the SMB and the batch processes, different definitions of the process performance parameters have to be defined for each process. The different definitions are defined as follows.

SMB separation. The specific productivity of compound i:

$$Pr_{SMB,i} = \frac{\dot{Q}_{Feed} c_{Feed,i}}{V_{ads}} \quad (12)$$

The specific eluent consumption of compound i:

$$Ec_{SMB,i} = \frac{\dot{Q}_{Feed} + \dot{Q}_{Eluent}}{\dot{m}_{A,i}} \quad (13)$$

Yield of compound i:

$$Y_{\mathrm{SMB},i} = \frac{\dot{m}_{A,i}}{\dot{Q}_{\mathrm{Feed}} c_{\mathrm{Feed},i}} \tag{14}$$

The mass flow of compound i in the extract or raffinate can be calculated by applying Eq. (15). A can represent the extract or raffinate flow as a function of where the product elutes:

$$\dot{m}_{A,i} = \frac{\dot{Q}_{A,i}}{t_{\mathrm{period}}} \int_{(n-1)t_{\mathrm{period}}}^{nt_{\mathrm{period}}} C_{A,i}(t)\,\mathrm{d}t \tag{15}$$

Batch separation. The specific productivity of compound i:

$$Pr_{\mathrm{SC},i} = \frac{V_{\mathrm{inj}} c_{\mathrm{Feed},i} Y_{\mathrm{SC},i}}{t_{\mathrm{cycl}} V_{\mathrm{ads}}} \tag{16}$$

The specific eluent consumption:

$$Ec_{\mathrm{SC},i} = \frac{\dot{Q} t_{\mathrm{cycl}}}{V_{\mathrm{inj}} c_{\mathrm{Feed},i} Y_{\mathrm{SC},i}} \tag{17}$$

Yield of compound i:

$$Y_{\mathrm{SC},i} = \frac{m_{X,i}}{V_{\mathrm{inj}} c_{\mathrm{Feed},i}} \tag{18}$$

The mass $m_{X,i}$ of product i collected in fraction X is defined by Eq. (19). As shown in Fig. 2, X can represent fraction A or B:

$$m_{X,i} = \dot{Q} \cdot \int_{t_{SX}}^{t_{EX}} c_i(t)\,\mathrm{d}t \tag{19}$$

Calculation of the specific separation costs is complex due to various influencing parameters and cost structures. Therefore, we propose the following cost function which can be easily adapted to specific conditions.

The total separation costs can be divided into:

(a) *Separation problem independent costs*. The separation problem independent costs are specific for each company. They depend on the different fixed cost structures, for example overhead costs, wages and maintenance. Additionally, the capital costs are independent from the separation problem. The capital as well as the maintenance and labour costs can be expressed in costs per hour of operation if only a small number of separation campaigns are carried out during a year. If the total number of different separations is too high, a significant time of the year has to be spent on change-over times. In this contribution we assume that it is possible to express all cost contributing parameters as a linear function of the operating time.

(b) *Separation problem dependent costs*. The separation problem dependent costs are directly correlated to a given separation problem and the amount of substance which has to be produced. This includes the costs for eluent, adsorbent and lost feed.

The capital costs per operating hour $C_{\mathrm{cap}}^{\mathrm{h}}$ depend on the investment costs C_{invest}, the number of years of depreciation $n_{\text{write-off}}$, and the maximum operating hours per year $t_{\mathrm{oper}}^{\mathrm{max}}$. To calculate the total capital costs of the separation only the operating time t_{oper} of the separation has to be known:

$$C_{\mathrm{cap}} = \frac{C_{\mathrm{invest}}}{n_{\text{write-off}} t_{\mathrm{oper}}^{\mathrm{max}}} \cdot t_{\mathrm{oper}} = C_{\mathrm{cap}}^{\mathrm{h}} t_{\mathrm{oper}} \tag{20}$$

The costs of labour and maintenance (operation costs) C_{oper} are assumed to be independent from the plant size and dependent on the total operating time of the plant. Therefore, they are expressed by applying a cost factor per operating hour $C_{\mathrm{oper}}^{\mathrm{h}}$:

$$C_{\mathrm{oper}} = C_{\mathrm{oper}}^{\mathrm{h}} t_{\mathrm{oper}} \tag{21}$$

The separation problem dependent costs are determined by applying the process performance parameters and the required production amount $m_{\mathrm{prod},i}$ of compound i. The operating time can be calculated from the required production amount and the production rate $\dot{m}_{\mathrm{prod},i}$ of a given chromatographic unit.

The total eluent costs C_{el} are determined from the specific eluent consumption (batch or SMB), the production amount and the costs per volume of eluent f_{el}:

$$\begin{aligned} C_{\mathrm{el}} &= Ec_{\mathrm{SC/SMB},i} m_{\mathrm{prod},i} f_{\mathrm{el}} \\ &= Ec_{\mathrm{SC/SMB},i} \dot{m}_{\mathrm{prod},i} t_{\mathrm{oper}} f_{\mathrm{el}} \end{aligned} \tag{22}$$

The total costs of the adsorbent C_{ads} are defined from the number of column refills n_{refill}, the column volume, the costs per kilogram of adsorbent $f_{\mathrm{ads}}$and the apparent adsorbent density ρ_{app}. The number of column refills is calculated from the ratio of the required operating time and the lifetime of the

adsorbent t_{life}. If the adsorbent can be reused for further separations, the value of n_{refill} can be a non-integer:

$$C_{ads} = n_{refill} V_C \rho_{app} f_{ads} = \frac{t_{oper}}{t_{life}} \cdot V_C \rho_{app} f_{ads} \quad (23)$$

The column volume is calculated from the required production amount of compound i and the productivity (batch or SMB):

$$V_c = \frac{m_{prod,i}}{t_{oper}(1-\varepsilon_t) Pr_{SC/SMB,i}} \quad (24)$$

Consequently, the total adsorbent costs are defined as:

$$C_{ads} = \frac{m_{prod,i} \rho_{app} f_{ads}}{t_{life}(1-\varepsilon_t) Pr_{SC/SMB,i}} \quad (25)$$

The crude loss costs $C_{crudeloss}$ can also be calculated as a factor of the process performance parameter yield, the required production amount of compound i, the mass fraction of compound i in the feed $\chi_{Feed,i}$, and the costs per gram feed f_{feed}:

$$C_{crudeloss} = \frac{m_{prod,i}}{\chi_{Feed,i}} \cdot \left(\frac{1 - Y_{SC/SMB,i}}{Y_{SC/SMB,i}} \right) \cdot f_{feed} = \frac{\dot{m}_{prod,i}}{\chi_{Feed,i}} \cdot t_{oper} \cdot \left(\frac{1 - Y_{SC/SMB,i}}{Y_{SC/SMB,i}} \right) \cdot f_{feed} \quad (26)$$

The total separation costs C_{sep} are determined by considering the five cost contributions:

$$C_{sep} = C_{cap} + C_{oper} + C_{ads} + C_{el} + C_{crudeloss} \quad (27)$$

To compare the separation costs for different production scales the specific separation costs C_{sep}^{spec} are defined as:

$$C_{sep}^{spec} = \frac{C_{sep}}{m_{prod,i}} = C_{cap}^{spec} + C_{oper}^{spec} + C_{ads}^{spec} + C_{el}^{spec} + C_{crudeloss}^{spec} \quad (28)$$

$$C_{sep}^{spec} = \frac{C_{cap}^{h}}{\dot{m}_{prod,i}} + \frac{C_{oper}^{h}}{\dot{m}_{prod,i}} + \frac{f_{ads}\rho_{app}}{Pr_{SC/SMB,i} t_{life}(1-\varepsilon_t)} + Ec_{SC/SMB,i} f_{el} + \frac{f_{feed}}{\chi_{Feed,i}} \cdot \left(\frac{1 - Y_{SC/SMB,i}}{Y_{SC/SMB,i}} \right) \quad (29)$$

Applying Eq. (29), the specific separation costs for the complete operating regime can be estimated for the process performance parameters and a given production rate.

Besides these cost calculations, constraints have to be taken into account. These are the purity of the products as well as the maximum pressure drop. The pressure drop caused by the flow through a fixed bed can be expressed by correlation (30) proposed by Darcy et al. [27]:

$$\Delta p = \Psi \cdot \frac{u_{int} \eta_{fl} L_C}{d_p^2} \quad (30)$$

3. Materials and experimental design

In this contribution the separation of a racemic mixture of a precursor of a potent cardiotonic drug with Ca-sensitising activity from Merck (Darmstadt, Germany) was investigated. Nevertheless, the optimisation approach is applicable for most isocratic two-component chromatographic separations.

The model compound, EMD53986 (for structure, see Fig. 3), is an intermediate of a potent new cardiotonic drug with Ca-sensitizing activity. The enantiomers of the final drug EMD53998 exhibit different modes of action [31].

In a previous study the separation conditions of EMD53986 on different chiral stationary phases (CSPs) were examined and optimised [31]. The best results were obtained on amylose-tris(3,5-dimethylphenylcarbamate) (Chiralpak AD, Daicel) using 100% ethanol, gradient grade (Merck) as eluent.

Batch experiments were carried out on a chromatographic device, a NovaPrep Model NP 200 (Merck). The CSP with a mean particle diameter of 20 μm was packed into preparative columns (Self-

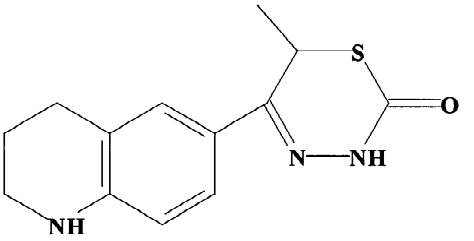

Fig. 3. Structure of EMD53986.

packer NW 25, Merck) of 25 mm I.D. at a bed length of 108 mm. The column temperature was adjusted to 25°C.

The SMB experiments were performed on a preparative SMB unit (LicosepLab, Novasep, Vandoevre-lès-Nancy, France). It consisted of eight double jacked HPLC columns (108×25 mm). The columns were thermostated and arranged in a 2:2:2:2 configuration. Fig. 4 shows a flowsheet of the SMB unit.

The concentration of both enantiomers was measured on-line using a two-detector system. The detectors were a polarimeter (PolarMonitor, IBZ Messtechnik, Hannover, Germany) and a UV detector (L7400, Merck–Hitachi, Darmstadt, Germany). Applying this technique provides on-line monitoring of single concentrations of the compounds, even in mixtures. The detectors are located on the suction side of the recycling pump. The calibration, experimental results and experience with this on-line monitoring device are presented in Ref. [22].

4. Results and discussion

4.1. Model parameters

The procedure to determine the model parameter as well as the complete set of model parameters are summarised in a previous paper [22]. The adsorption isotherms of EMD 53986 on Chiralpak AD were determined by evaluating breakthrough experiments. Here, a new technique of on-line monitoring of single concentrations is utilised to evaluate equilibrium data of the racemic mixture. This application ensures the accurate determination of adsorption isotherms with tolerable effort and high accuracy. The adsorption equilibria of EMD 53986 for the pure substances and the racemic (1:1) mixture are shown in Fig. 5. Besides the adsorption isotherms of the pure components, the isotherms of the racemic mixture (1:1 mixture) are also given. The adsorption behavior, especially of the (−)-enantiomer, is strongly non-linear. The adsorption of the (+)-enantiomer

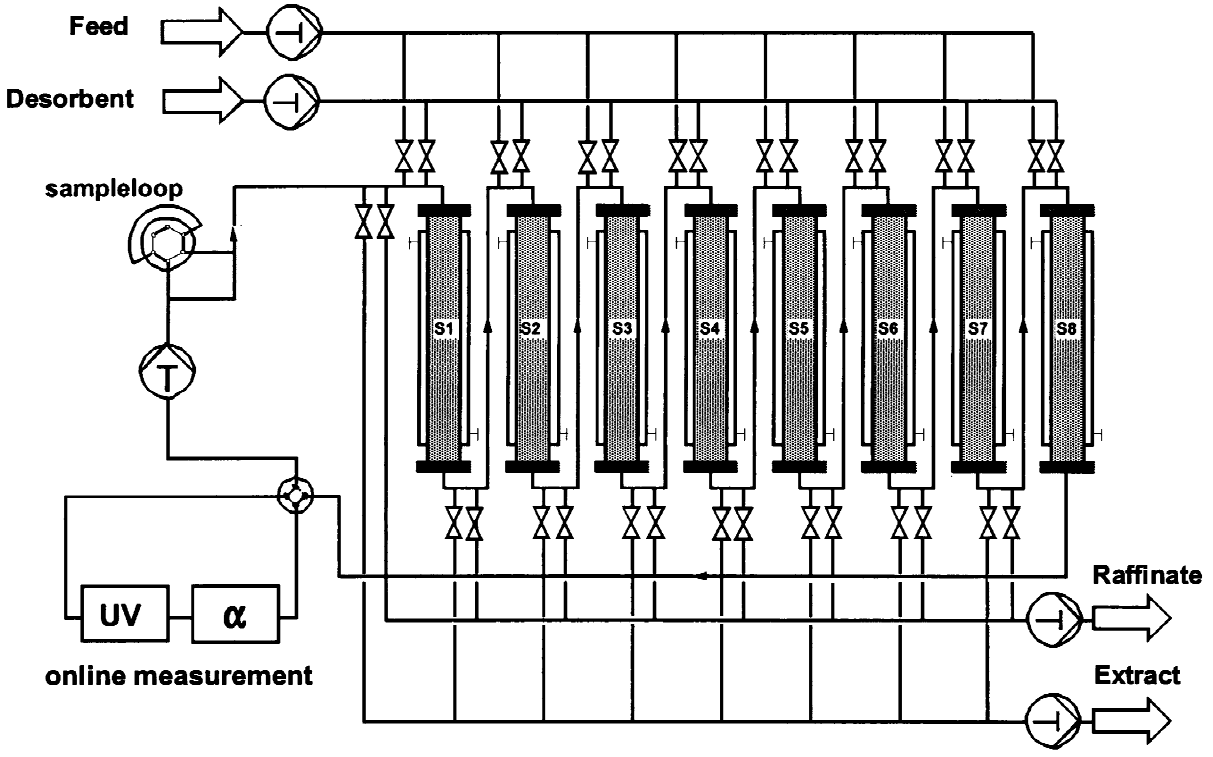

Fig. 4. Flowsheet of the SMB unit.

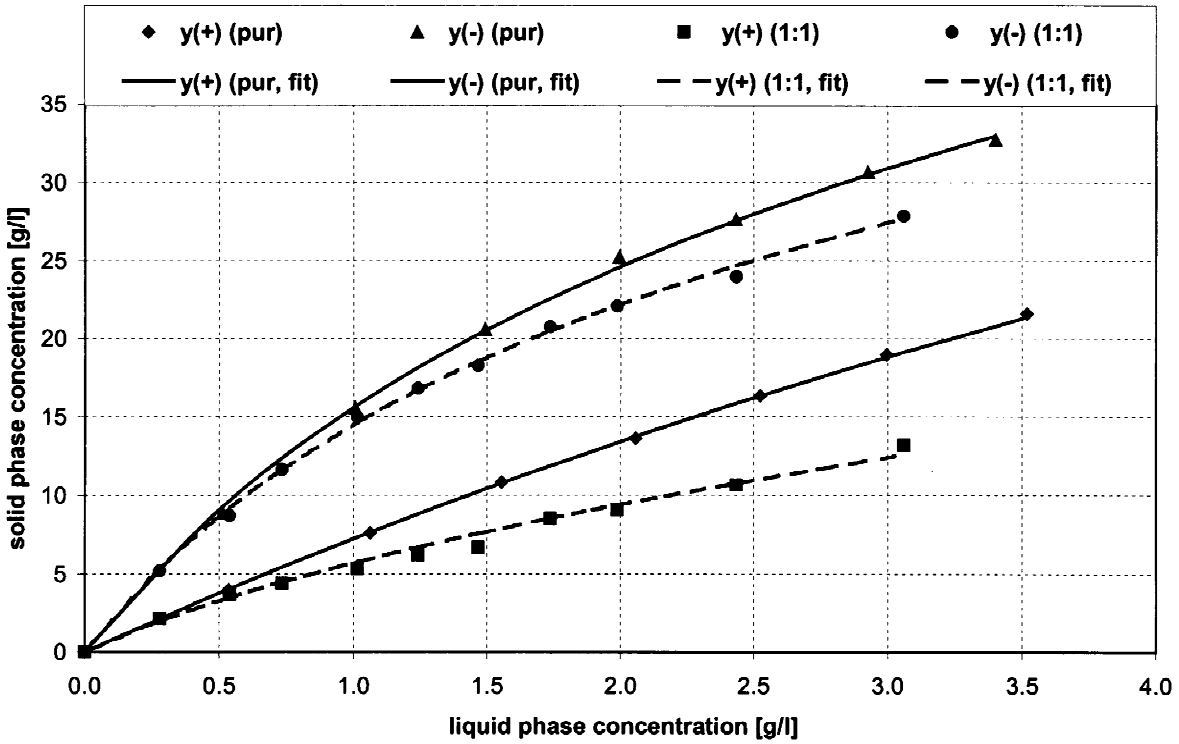

Fig. 5. Adsorption isotherms of EMD53986, measured and fitted data.

is more influenced by the (−)-enantiomer than the reverse case.

The experimental data were fitted to the modified competitive Langmuir model (Eqs. (31) and (32)). This adsorption isotherm model shows a concentration dependent selectivity:

$$y_{(+)} = 2.054c_{(+)} + \frac{5.847c_{(+)}}{1 + 0.129c_{(+)} + 0.472c_{(-)}} \quad (31)$$

$$y_{(-)} = 2.054c_{(-)} + \frac{19.902c_{(-)}}{1 + 0.129c_{(+)} + 0.472c_{(-)}} \quad (32)$$

Besides an excellent fit to the measured data this isotherm model provides the possibility to adjust a save operating point of the SMB process on the basis of the triangle theory proposed by Morbidelli et al. [28].

The HETP correlations for the enantiomers were determined as:

$$HETP_{(+)} = 0.05cm + 1.9su_{\text{int}} \quad (33)$$

$$HETP_{(-)} = 0.0126cm + 1.63su_{\text{int}} \quad (34)$$

As constraints for the optimisation, the product purities are fixed at 99.9%. The free parameter Ψ of the pressure drop correlation (30) was determined to be 1233.4.

4.2. Experimental validation of the process models

The experimental validation of the process models is described in detail in Refs. [22,23]. Fig. 6 shows the concentration profile for a breakthrough experiment on a single chromatographic column. The good agreement between experimental and simulated results is remarkable.

Several SMB experiments were carried out in order to validate the proposed SMB process model with on-line measured concentration profiles providing a high data density. The operating parameters are summarised in Table 1.

Fig. 7 shows the concentration profiles determined

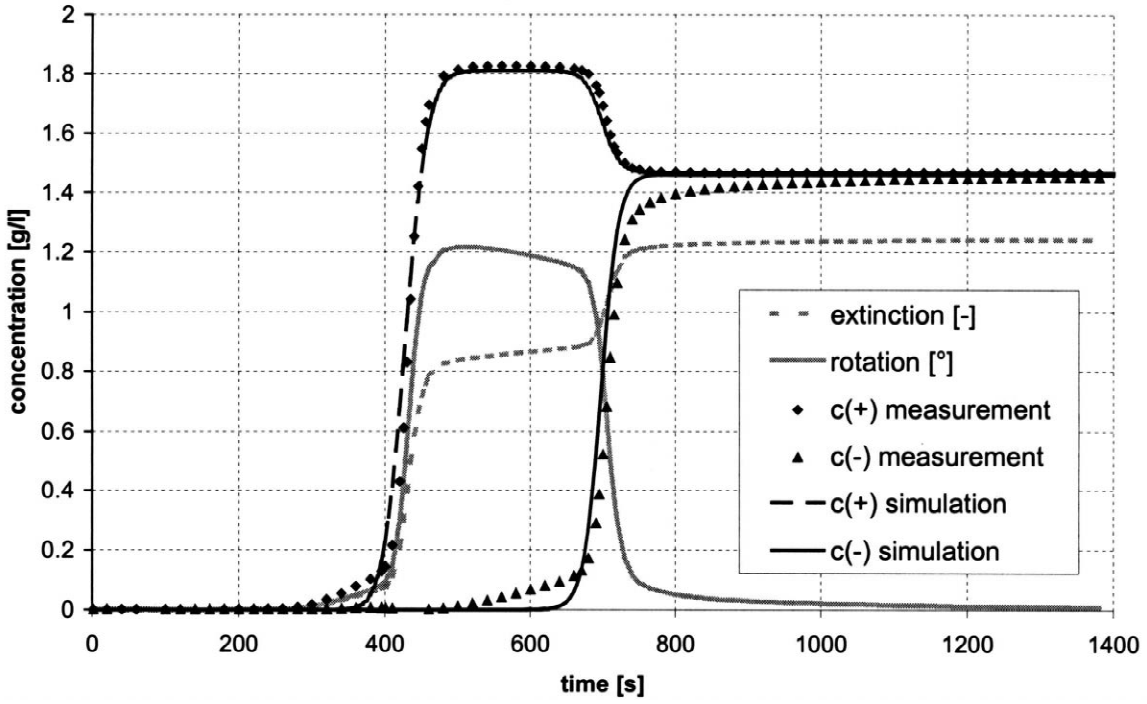

Fig. 6. Breakthrough experiment for EMD53986, racemate concentration 3 g/dm^3.

by the on-line monitoring system and the simulation results. Very good agreement between experimental and simulation results can be observed. Also, it is worth mentioning that all model parameters were determined in previous batch experiments on a separate column. Due to the consistency of the parameter determination concept and the high accuracy of the model parameters, no further fit of parameters to the SMB results was necessary to achieve this excellent conformity. The purities of the extract and raffinate were determined to be higher than 99.9% for the experiment and simulation results.

4.3. Development of design optimisation strategies

This experimentally validated process model, which is valid in a wide range of possible operating regimes, provides the possibility to carry out simulation studies to optimise the operation and design conditions for a batch as well as for a SMB process.

As described in the Theory section it is possible to calculate the specific separation costs for every set of operating parameters if the process performance parameters and the required production amount are given. A large number of simulations were carried out to calculate the process performance parameters

Table 1
Operating parameters of a SMB experiment

Feed (cm^3/min)	Desorbent (cm^3/min)	Raffinate (cm^3/min)	Extract (cm^3/min)	Recycling (cm^3/min)	Shifting time (s)	Feed conc. (g/dm^3) (racemate)
5.54	57.49	15.06	47.97	72	431	5

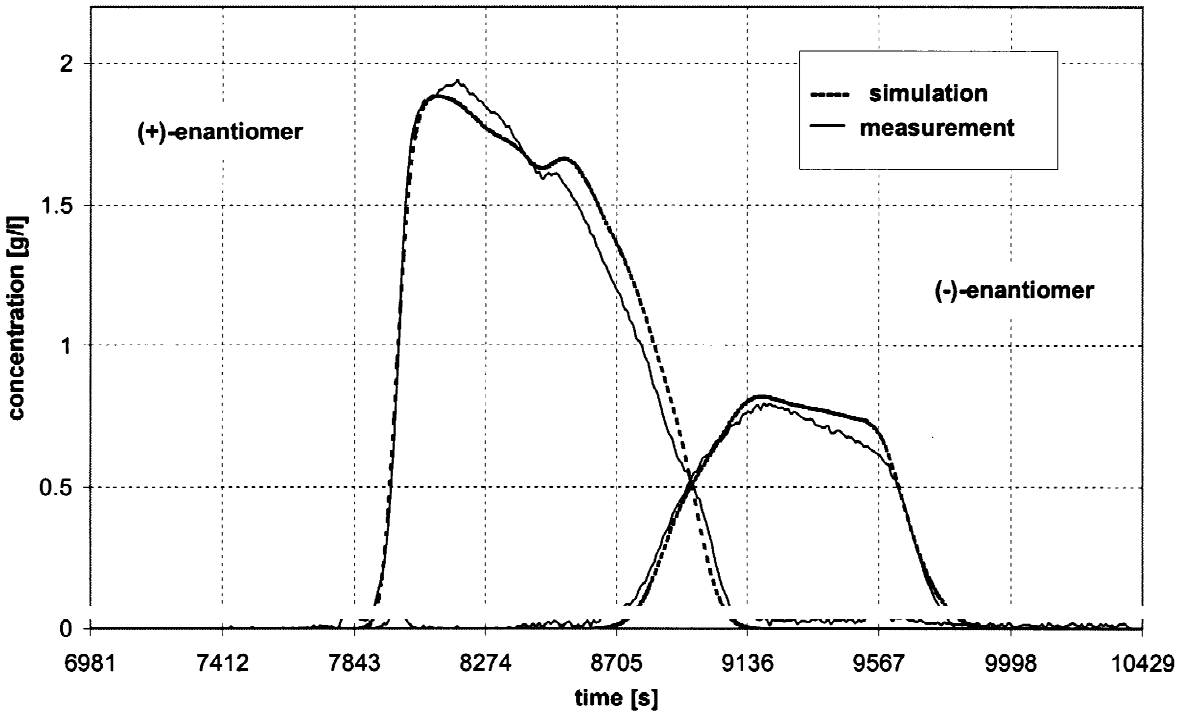

Fig. 7. Comparison of the experimental and simulated results for the SMB experiment for EMD53986.

as well as the specific separation costs as a function of the operating parameters. A major problem is the large number of influencing parameters for design optimisation. Therefore, it is necessary to reduce the complexity of the problem by introducing dimensionless numbers which represent real degrees of freedom.

4.4. Optimisation strategy for batch chromatography

For batch chromatography, the flow-rate, the injection time, the column length and the cut times have to be adjusted. To fulfill the purity constraint, four cut times are necessary.

The remaining three operating parameters, flow-rate, column length and injection time, cannot be varied independently. The column length and flow-rate influence the efficiency of the column. The amount of feed which is introduced per column volume depends on all three parameters. Felinger and Guiochon [2,7–9] proposed the choice of the number of plates (Eq. (11)) and the loading factor (Eq. (35)) as independent optimisation parameters:

$$L_{\mathrm{f}} = \frac{m_{\mathrm{inj}}}{m_{\mathrm{capacity}}} = \frac{c_{\mathrm{Feed},i} V_{\mathrm{inj}}}{y_{\max} V_{\mathrm{C}} (1 - \varepsilon_{\mathrm{t}})} \tag{35}$$

From analysis of the partial differential equation (2) (PDE) describing the column dynamics it is obvious that the two dimensionless numbers, Peclet (Eq. (6)) and Stanton (Eq. (5)), are the only parameters that influence the solution of the PDE and thus determine the column efficiency. It is also evident that, for linear chromatography, it is sufficient to express them in terms of the plate number of compound i (Eq. (10)). Therefore, we further assumed that the plate number of compound i and the loading factor are sufficient to completely characterise the chromatogram in non-linear chromatography.

To prove this assumption, several simulations for different column lengths, flow-rates and injection volumes, but with the same numbers of stages N_i and loading factor L_{f}, were carried out. Furthermore, it was assumed that the number of plates in the system

can be calculated from the plate height correlation (Eq. (33)) of the lower absorbable (+)-enantiomer. The resulting chromatograms are plotted over a reduced time scale t/t_0 in Fig. 8.

The resulting chromatograms are nearly identical. This proves the assumption that the dimensionless numbers loading factor L_f and plate number N_i are the only independent optimisation parameters in nonlinear chromatography. It is worth mentioning that the simulations were carried out by applying the complete validated process model. However, it is not advisable to use a plate model to simulate a chromatographic process. This results from the fact that every single component requires an individual number of plates to be properly modelled, which cannot be realised with a plate model. But the number of plates of the second compound could also have been applied to characterise the column efficiency. The only difference is the resulting number of plates. The plate number of one component can be used to characterise the efficiency of the column only.

Therefore, it is possible to calculate all process performance parameters of batch separations as a function of these characteristic dimensionless numbers, independent of the scale of the separation or the individual column geometry. The results are illustrated in three-dimensional diagrams (Fig. 9). From these diagrams the effects that influence the performance and the costs of the separation are clearly presented.

Fig. 9a plots the productivity in grams enantiomer per volume of adsorbent and hour against the number of plates and the loading factor. The highest productivity is achieved for plate numbers of 40 and loading factors greater than one. For small loading factors, only very poor productivities can be realised. This results from the very small amount of material which is injected into the column. Fig. 9c illustrates that, in this case, the yield increases to about 100%, which means nearly baseline separation between the two peaks. As mentioned before, Fig. 9 demonstrates that optimum productivity and economy will not be found by applying cut strategy II of Fig. 2 without the collection of a waste fraction. The slight decrease

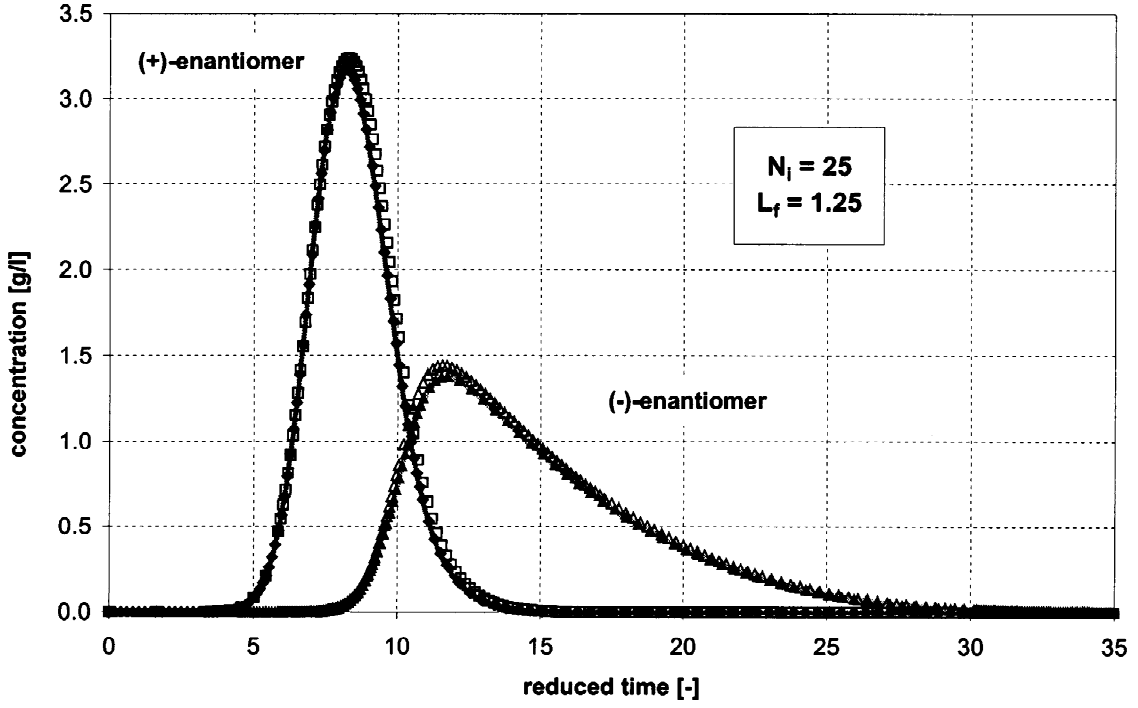

Fig. 8. Batch chromatogram for different operating and design parameters and constant number of plates ($N_i = 25$) and loading factor ($L_f = 1.25$) plotted over a reduced time scale.

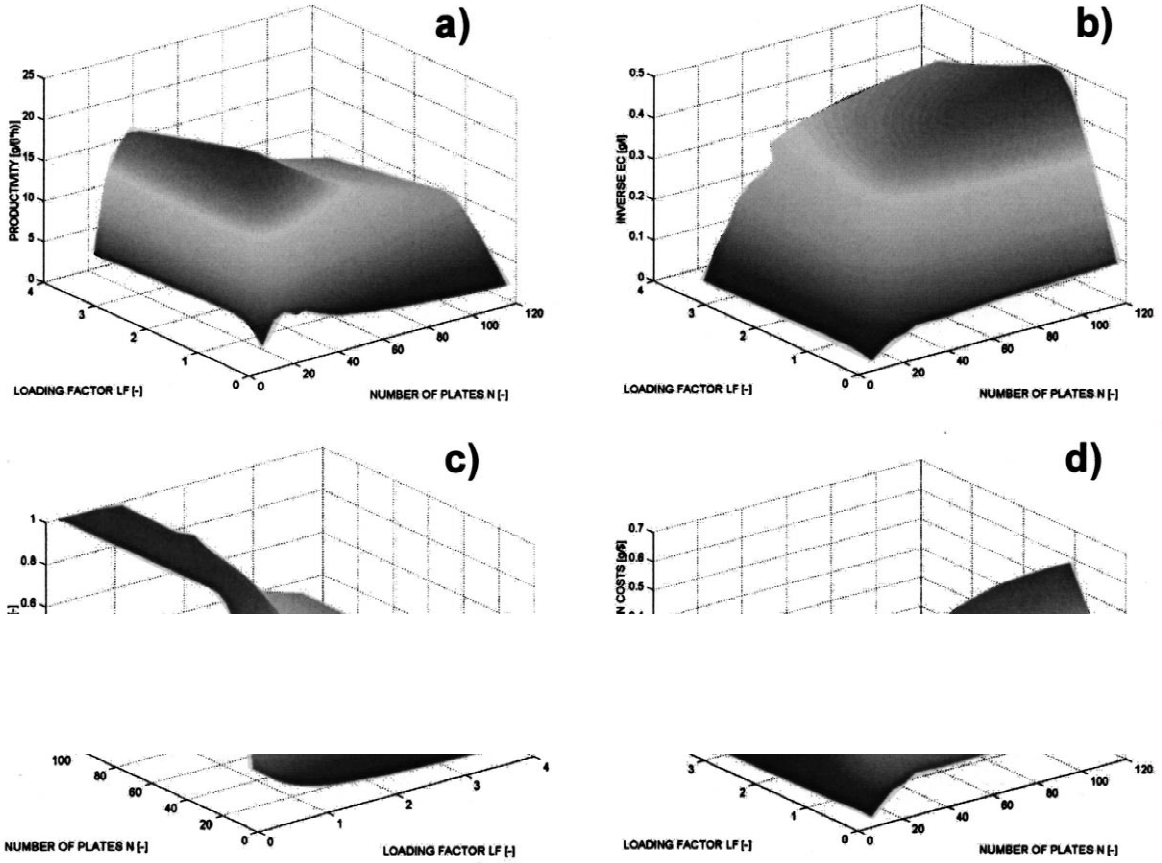

Fig. 9. Process performance and separation costs of batch chromatography, 99% purity.

in productivity for a further increase of the loading factor results from the strong decline in the yield. It can also be seen that increasing the plate number causes a strong increase of the productivity until the optimum is exceeded. A further increase in the number of plates causes a smooth decrease of the productivity.

The decrease in the yield with increasing loading factor is due to overlapping peaks. In this case, the purity constraint can only be fulfilled by collecting a large waste fraction. The yield decrease for very low plate numbers results from the influence of band broadening and therefore a larger waste fraction to fulfill purity demands.

Fig. 9b plots the *inverse specific eluent consumption* in grams enantiomer per volume eluent against the plate number and the loading factor. In contrast to the productivity, a constant decrease of the specific eluent consumption can be observed for an increase of the number of plates. But, similar to the productivity, the minimum values of the specific eluent consumption are achieved for loading factors greater than one. Also, a steep increase of the specific eluent consumption can be observed for small loading factors, which is equivalent to a nearly complete baseline separation of the peaks without a waste fraction. This results from the strong decrease of material per injection, which cannot be compensated by the small decrease in the cycle time.

Fig. 9d presents the *inverse specific separation costs* plotted against the number of plates and the loading factor. These costs were determined by applying Eq. (29) and the data summarised in Table 2. It becomes obvious that minimum separation costs are not located at the maximum productivity only. Eluent consumption and yield have to be taken into

Table 2
Data for operating costs calculation

	SMB		Batch	
	1000 kg/year	5000 kg/year	1000 kg/year	5000 kg/year
Column diameter (cm)	25.5	57	32	70
Column length (cm)	4.9	4.9	64	67
Configuration	2:2:2:2	2:2:2:2	–	–
Mass adsorbent (kg)	11.4	57.0	29.4	147.5
Yield (%)	100	100	96.15	96.15
Spec. productivity (g dm^{-3} h^{-1})	10.06	10.06	8.70	8.70
Spec. eluent consumption (dm^3/g)	2.83	2.83	2.24	2.24
Spec. adsorbent costs[a] (US$/kg)	13 453	13 453	13 453	13 453
Spec. eluent costs[a] (US$/$dm^3$)	0.47	0.47	0.47	0.47
Spec. feed costs[a] (US$/g)	7.17	7.17	7.17	7.17
App. adsorbent density (kg/dm^3)	0.572	0.572	0.572	0.572
Adsorbent lifetime[a] (h)	7000	7000	7000	7000
Total porosity	0.72	0.72	0.72	0.72
Operation time (h)	8000	8000	8000	8000
Max. op. time per year (h/year)	8000	8000	8000	8000
Years of depreciation (years)	4	4	4	4
Operation costs per hour[a] (US$/h)	22.4	22.4	22.4	22.4
Investment costs[a] ($\cdot 10^6$ US$)	1.59	3.18	0.73	1.64
Spec. separation costs (US$/g)	2.11	1.72	2.18	1.94

[a] Estimated.

account. Further, the contradiction between minimising the eluent costs and maximising the productivity is worth mentioning. High productivity requires a small number of plates. In contrast, low specific eluent consumption requires a large number of plates. As a result, the economic optimum is a compromise between these contradictory requirements.

The column design can be adjusted by applying the required production rate, the pressure drop correlation (Eq. (30)), the plate height correlation of one compound (Eq. (33)) and the plots of process performance in Fig. 9a–c. The algorithm for the economic optimal design of a batch separation is shown in Fig. 10.

The algorithm starts with an initial guess for the column design. Also, the maximum pressure drop has to be adjusted to obtain an initial guess for the investment costs. The estimated investment costs, the specific cost factors for adsorbent, feed and eluent and the performance plots in Fig. 9 are applied to calculate the specific separation costs for every operating point using Eq. (29). As a result, the plate number and loading factor for minimum costs are adjusted. The constant term in Eq. (11) can be neglected if the contribution of dispersion to the total plate height is small, which is true for high interstitial velocities and particles which are not too small. In combination with the pressure drop correlation (Eq. (30)) the optimal interstitial velocity is determined from the optimal number of plates. Then the length of the column is adjusted for this interstitial velocity and the maximum pressure drop. Together with the required production rate the column diameter is calculated. Now, a new optimal design of the column is fixed and is compared with the initial or previous design. If necessary, a new value for the investment costs is estimated and the procedure is repeated until the design parameters converge. To check the influence of a different column design, for example with different pressure drops, the algorithm has to be carried out for further values of the maximum pressure drop.

4.5. Optimisation strategy for SMB chromatography

In the following, a procedure for the complete

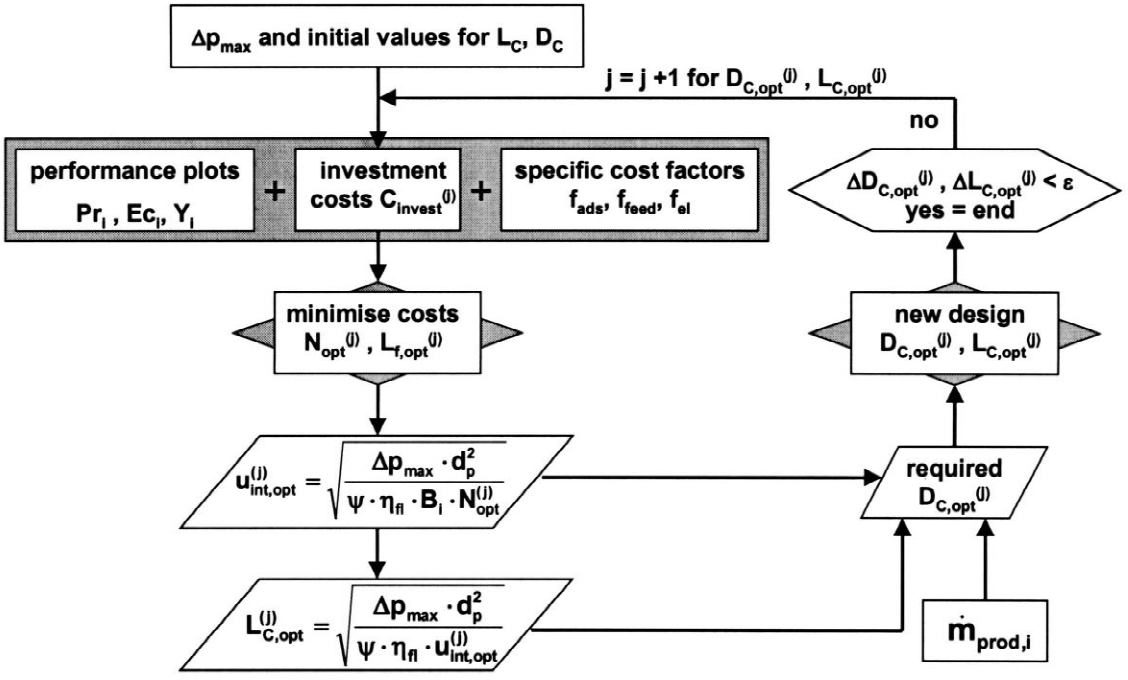

Fig. 10. Algorithm for a complete design of batch chromatography.

design of a SMB unit is presented. The influence of the column length is the main topic. However, the number of columns is fixed to two columns per zone. An optimisation of this so-called segmentation is the topic of a following paper.

Before focussing on the design parameters, the method to optimise the operating parameters will first be illustrated briefly. As objective function, the specific productivity will be discussed first. To achieve pure products and high productivity, the flow-rates in all four sections have to be chosen in such a way that the fronts and rears of the concentration profiles are at specific locations at the end of an injection period. Fig. 11 shows a simplified optimal internal concentration profile. Furthermore, the four stopping points for the concentration profiles as constraints for the optimisation are presented.

For a given set of design parameters, the flow-rate in zone I, generally the zone with the highest flow, is fixed, usually at its maximum related to the maximum allowable pressure drop in the unit. It will be demonstrated later that fixing at the maximum is not necessary to achieve optimal process performance. Fixing the flow-rate in zone I means fixing one of the five free operating parameters. Based on the triangle theory [12,14,28], an initial guess of the four flow-rate ratios m_j is done considering a safety margin of about 10%. This starting point is illustrated in the operating diagram for EMD53986 in Fig. 12. According to the simplified model assumptions (TMB model and equilibrium theory) the theoretical optimum is located at the vertex of the triangle, due to the largest difference between the flow-rate ratios of zone II and III and with that the highest feed flow.

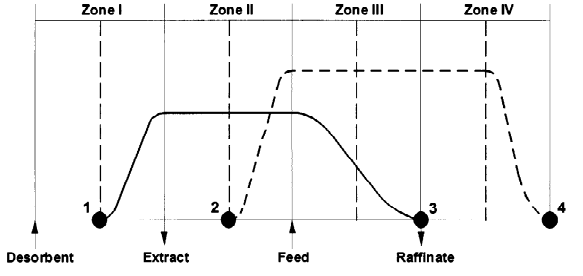

Fig. 11. Optimal internal SMB concentration profile at the end of an injection period.

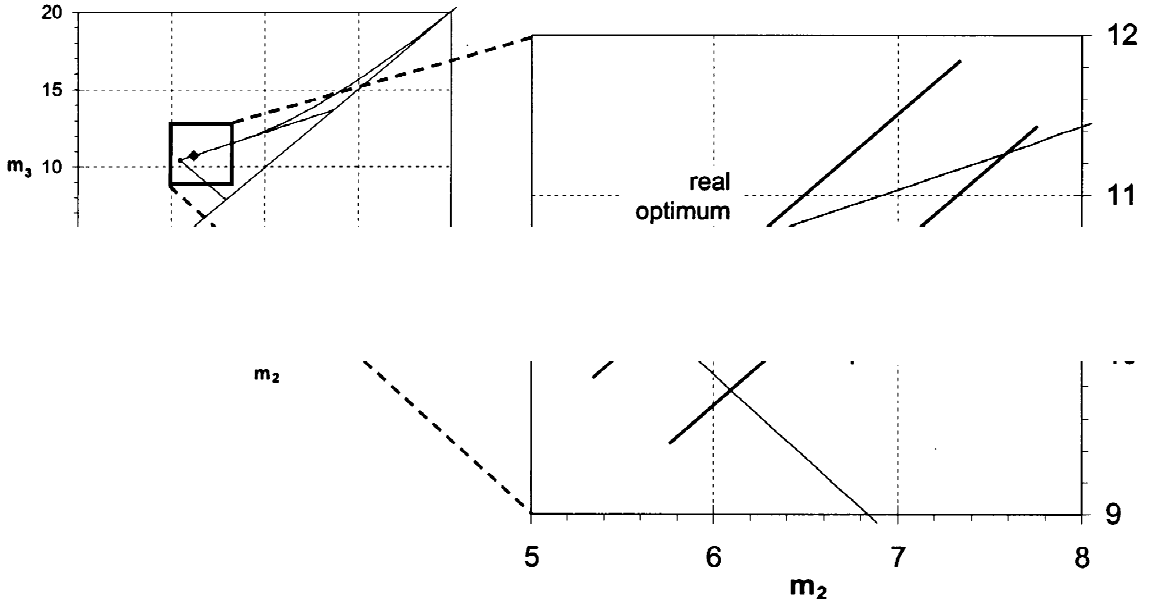

Fig. 12. Operating diagram for EMD53986; strategy for the operating parameter optimisation.

Nevertheless, it is worth mentioning that the theoretical optimum does not lead to pure products, so that a safety margin is always required.

In the second step a systematic simulation study applying the complete and experimentally validated SMB process model is performed [18,29] considering all operating parameters. However, the most difficult step is to adjust the flow-rate ratios in zone II and III, especially for strong non-linear isotherms with interactions as in the case of EMD53986. Therefore, the m_2–m_3 plane is divided into segments by lines parallel to the diagonal. Each line symbolises a constant feed flow. For a safe starting point, the location of the concentration profiles, the purities and productivity are calculated by dynamic simulation. If the purity of the external streams is higher than demanded or if there is enough space between the fronts and rears of the profiles to the stopping points (see Fig. 11), the next step is to increase the feed flow, which means jumping to a parallel line closer to the vertex. If, after a new simulation, the purity of one compound is too low, the operating point has to be varied along the parallel line until the purity of both streams is nearly equal. If the purities are still too high the next increase of the feed flow can be performed. Otherwise, if both purities are too low the feed flow has to be decreased. Application of this systematic procedure leads to the real optimal operating point (Fig. 12) for the fixed flow-rate in zone I and the given set of design parameters. This procedure can be repeated for different flow-rates in zone I. Additionally, this method is also applicable for other objective functions such as the separation costs. In contrast to the similar method proposed by Biressi et al. [30], it is necessary to mention here that a complete SMB model is applied and, furthermore, all operating parameters are considered. Biressi et al. vary the flow-rates in zones II and III only.

Moreover, an algorithm for the automated calculation of optimum operating conditions considering this detailed SMB and different objective functions has been tested successfully [18,19].

In the following we will focus on the influence of the column length. The column diameter ($D_c = 2.5$ cm) is assumed to be a scale parameter. Fig. 13 plots the productivity over the length of one chromatographic column of the SMB unit for two different flow-rates, $\dot{Q}_{I(1)} = 1.5$ cm^3/s and $\dot{Q}_{I(2)} = 1.7$ cm^3/s, in zone I. For each column length the four free operating parameters, the four flow-rate ratios m_j,

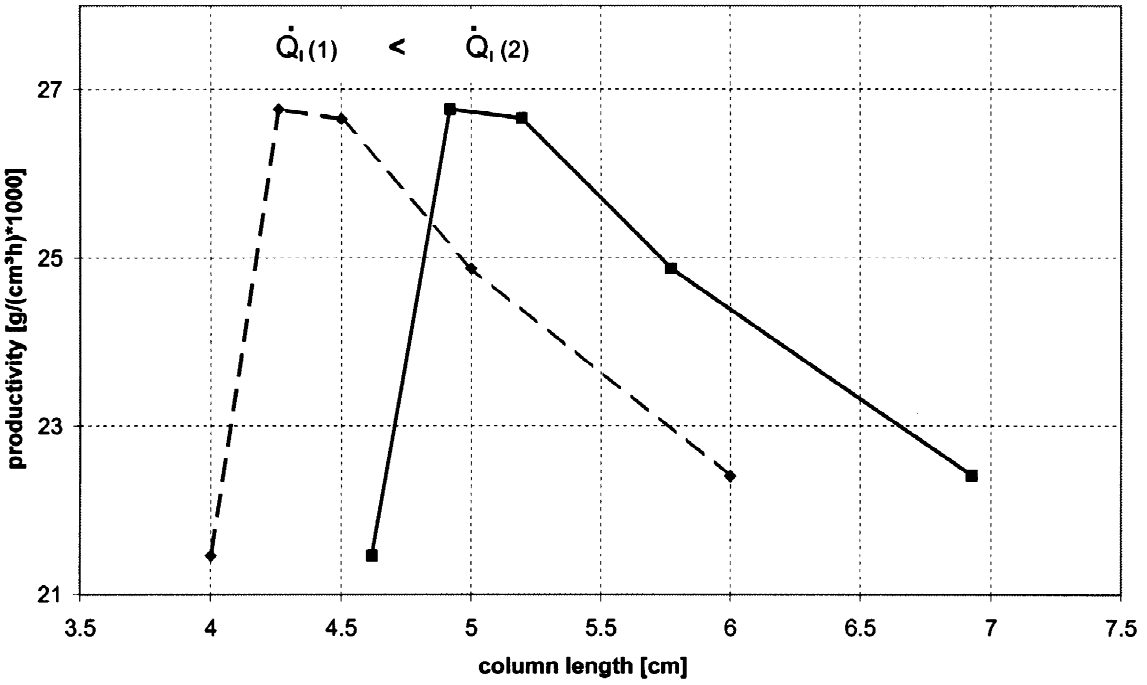

Fig. 13. Influence of the column length on the productivity for two different flow-rates.

have been optimised, achieving maximum productivity. The maximum pressure drop was ignored in this study.

From Fig. 13 it becomes clear that, for each given flow-rate in zone I, an optimal column length with a maximum productivity can be found. Further, the productivity curves are almost parallel shifted so that the maximum productivities for both flow-rates are the same. The higher the flow-rate is fixed the longer the column has to be to reach maximum productivity.

Now we come to the influence of the pressure drop. Biressi et al. [30] proposed to fix the flow-rate in zone I at its maximum due to the maximum allowable pressure drop. We found that, for two different pressure drops, two different column lengths, but the same maximum productivity, result. The maximum productivity is not necessarily located at the maximum pressure drop. Additionally, a high pressure drop increases the investment cost of a chromatographic unit drastically. Therefore, it is not advisable to fix the maximum pressure drop too high and too early in the design procedure.

Besides, fixing the column length for a separation problem too early can also cause a dilemma. If the column length is too long the optimum productivity cannot be reached due to the pressure drop restriction. For example, with a column length of 6 cm and a maximum flow of 1.7 cm^3/s the maximum productivity cannot be reached due to the pressure drop restriction (see Fig. 13). The required flow-rates to achieve maximum productivity cannot be realised. The only way to solve this problem is to reduce the column length. In our opinion, this bottleneck can often be observed in preparative chromatographic separations. As a consequence, it is necessary to optimise the column length and the flow-rate in zone I simultaneously considering the pressure drop.

Now we focus on how to solve this dilemma. Concentrating again on Fig. 13, we find that for both maximum productivities the numbers of theoretical plates N_i per zone are equal, although the flow-rates and the column lengths are different. Further, the four flow-rate ratios m_j are also equal. As a result it should be highlighted that, for a design optimisation of a SMB separation, only five dimensionless param-

eter are sufficient. These are the number of theoretical plates N_i and the four flow-rate ratios m_j.

Comparable to batch chromatography, nearly identical concentration profiles can be observed if the flow-rate ratios, the numbers of plates per zone and the feed concentration are kept constant. The resulting axial profiles are plotted over the reduced length scale L_C/L_{ges} in Fig. 14.

This result can be observed only if band broadening in the chromatographic system is dominated by the mass transfer resistance, e.g. if the particle diameter and the interstitial velocity are not too small. Otherwise, only one of the numbers of plates can be kept constant if the geometry and operating conditions are changed. Nevertheless, the reduction of complexity and number of influencing parameters in the optimisation problem justifies this simplification.

To illustrate the deviations from equilibrium theory, Fig. 15 plots in an operating diagram the flow-rate ratios of zones II and III for the five investigated column lengths (4, 4.25, 4.5, 5 and 6 cm) and the flow-rate $\dot{Q}_{I(1)}$ of Fig. 13. It is clear that, for each given column length or plate number, a certain optimal operating point can be determined. With decreasing column length (plate number) the optimal operating points move further away from the theoretical optimum inside the triangle. This behaviour demonstrates the increasing influence of the finite efficiency of chromatographic columns on the optimisation of the unit design.

Fig. 16 shows the algorithm for the complete design of a chromatographic SMB process. This algorithm is applicable for both objectives, specific productivity and specific separation costs.

Starting with initial values for the number of plates N_i and the four flow-rate ratios m_j, a dynamic simulation with the complete SMB model is performed. In the inner loop the optimisation of the operating parameters m_j for a given plate number is realised based on the strategy explained at the beginning of the next section. The outer loop con-

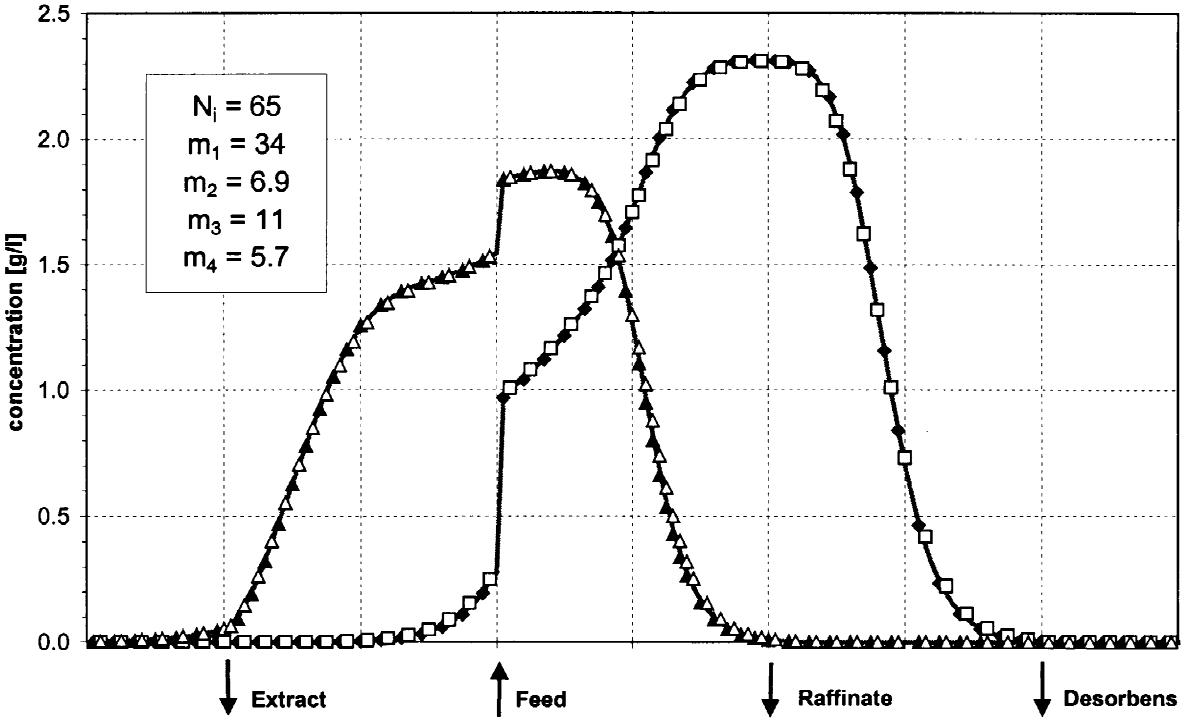

Fig. 14. Internal SMB concentration profiles for different operating parameters but constant flow-rate ratios and number of plates per zone plotted over a reduced length scale.

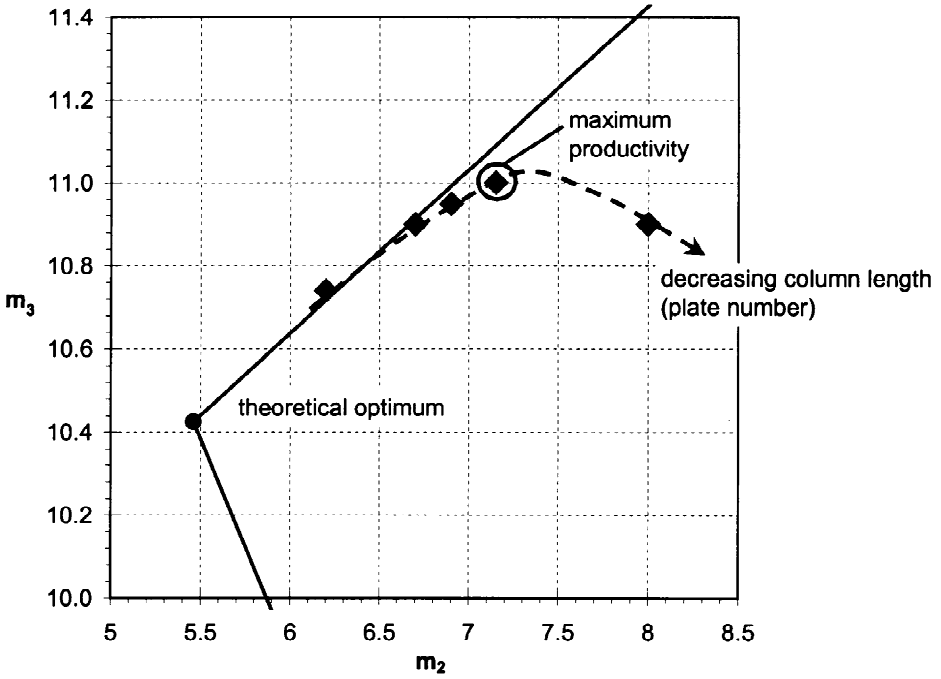

Fig. 15. Operating diagram with operating points for the five investigated column lengths (4, 4.25, 4.5, 5 and 6 cm).

centrates on the variation of the number of plates so that a wide range will be investigated.

This algorithm can be applied for different particle diameters and numbers of columns per zone. These results will be introduced in a following paper.

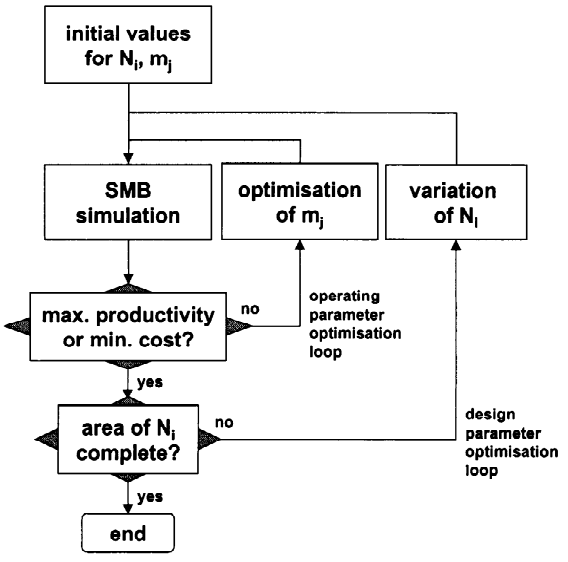

Fig. 16. Algorithm for a complete SMB design optimisation.

Applying the proposed algorithm, we obtain the dependence of the specific productivity, specific eluent consumption and specific separation costs shown in Fig. 17. Here, the specific costs for two different production rates, 1000 and 5000 kg/year, were determined. As mentioned before the productivity has a maximum at about 23 plates. For higher plate numbers the curve decreases. The eluent consumption has its maximum at the lowest plate number and decreases with increasing plate number. The specific separation costs for both production rates increase with decreasing plate number and increasing productivity. They are relatively high at the maximum productivity. This correlation is due to the high eluent consumption at low plate numbers. The minimum in separation costs is reached in a wide range of 30 to 45 plates. We further found that the cost increases smoothly with number of plates greater than 55.

Here, the contradiction between maximum productivity and minimum eluent consumption can again be found, as for batch chromatography. Optimising

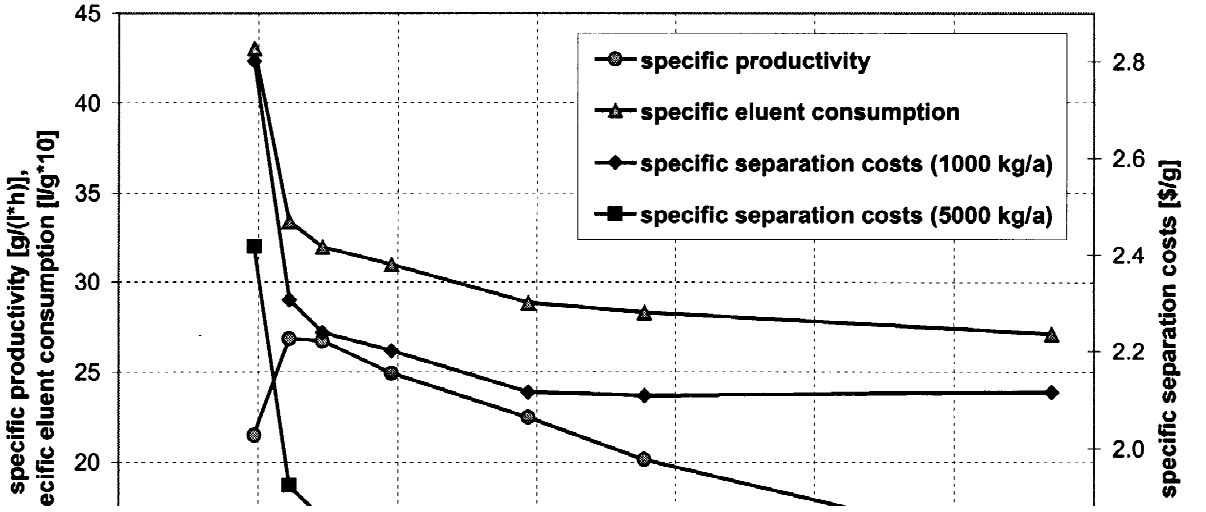

Fig. 17. Influence of the plate number on the specific productivity, specific eluent consumption and specific separation costs.

the productivity does not lead to minimum separation costs. The economic optimum is a compromise between contradictory parameters. Due to the influence of overhead costs the separation costs are higher for a production rate of 1000 kg/year than for 5000 kg/year. The curves are nearly parallel shifted.

After determination of the dimensionless parameters, the four flow-rate ratios m_j and the total number of plates, it is possible to determine the optimal column diameter and length for a given feed stream. In this context it is important to mention that no further simulations are required to specify the column geometry.

First, the correlations between the internal and the external flow-rates have to be established. They are derived from balances around the different nodes of the SMB unit:

$$\dot{Q}_{\mathrm{I}} = \dot{Q}_{\mathrm{IV}} + \dot{Q}_{\mathrm{Eluent}} \tag{36}$$

$$\dot{Q}_{\mathrm{II}} = \dot{Q}_{\mathrm{I}} + \dot{Q}_{\mathrm{Extract}} \tag{37}$$

$$\dot{Q}_{\mathrm{III}} = \dot{Q}_{\mathrm{II}} + \dot{Q}_{\mathrm{Feed}} \tag{38}$$

$$\dot{Q}_{\mathrm{IV}} = \dot{Q}_{\mathrm{III}} + \dot{Q}_{\mathrm{Raffinate}} \tag{39}$$

The following design strategy is similar to the strategy for batch chromatography illustrated in Fig. 10. For an initial guess of the column diameter, the corresponding column length can easily be calculated by applying Eqs. (36)–(39) together with the flow-rate ratios m_j (Eq. (1)) and the Van Deemter correlation (Eqs. (33) and (34)). Based on this specified column length and the internal flow-rates, the total pressure drop (Eq. (30)) can be determined. If the calculated pressure drop exceeds the allowed pressure drop, a larger diameter has to be chosen.

This procedure leads to one $L_{\mathrm{C}}/D_{\mathrm{C}}$ ratio that exactly fulfills the maximum pressure drop condition for the given feed stream. Certainly, smaller $L_{\mathrm{C}}/D_{\mathrm{C}}$ ratios are also applicable to reach the same optimal performance of the SMB plant, but with a lower pressure drop. It is worth mentioning that a lower pressure drop will decrease the investment cost of a chromatographic unit. However, the smaller the ratio becomes and the lower the pressure drop, the shorter

the same order of magnitude as the total eluent costs for SMB units. For higher production rates the proportional contribution of the costs for eluent, loss of feed and adsorbent increases, in contrast to the decrease of the relative costs for investment, maintenance and labour. Due to the smaller influence of costs for capital, labour and maintenance the contribution of eluent costs increases from 49.1 to 55.3% for batch and from 64.1 to 78.4% for SMB units, although the total eluent costs remain almost constant.

The solubility of the racemic mixture EMD53986 in ethanol is about 6 g/dm^3. Therefore, the contribution of eluent costs is relatively high. In general, higher solubilities lead to higher separation efficiency [34]. Further, the influence of the capacity of the stationary phase and the adsorbent costs increase and can become a limiting factor. For these cases, the productivity becomes more important and, consequently, the SMB technique becomes more advantageous in comparison with batch separation.

In this work the purity demand for SMB separation was 99.9% for both enantiomers. Consequently, the yield was almost 100%. If one enantiomer would be the target product only and a certain loss of feed would be possible, a further increase of the efficiency or decrease of the separation costs will be found.

5. Conclusion

In this work an effective strategy for the optimal choice of all process parameters (operation and design parameters) for chromatographic batch and SMB units is proposed. The main idea of this strategy is to introduce and optimise dimensionless process parameters to reduce the number of influencing parameters and apply a detailed and experimentally validated process model. The influencing dimensionless process parameters are the number of theoretical plates N_i and the loading factor L_f for batch chromatography and the plate number N_i and the four flow-rate ratios m_j of the four different zones for SMB units.

Furthermore, we show that the minimum separation costs for both units are not located at maximum productivity. Maximising the productivity does not lead to an economic process performance. The economic optimum is a compromise between the contradictory objectives of minimising the eluent consumption and maximising the productivity. Therefore, the choice of objective function is an important aspect for the optimisation of chromatographic processes.

It is also shown that the widespread opinion that optimal process performance is found at the maximum pressure drop only does not hold. In contrast, there is an infinite choice of design and operating parameters to achieve maximum productivity not at the maximum pressure drop only. Further, it is worth noting that a high pressure drop causes high investment costs. Thus, it is advisable to consider the influence of the pressure drop on the investment cost and not to fix the pressure drop too high.

In particular, we demonstrated that a cut strategy for batch chromatography considering a waste fraction, which means accepting a certain loss of feed, leads to optimum process performance. A yield restriction of 100% increases the separation costs drastically and for this reason this restriction is not advisable for batch chromatography.

Finally, we present an economic comparison of completely optimised batch and SMB processes for the separation of a racemic mixture (EMD53986, Merck, Germany) considering a cost function. The separation costs are almost equal for a low production rate (1000 kg/year). At a higher production rate (5000 kg/year) the separation costs of the batch unit are only 13% higher than that of the SMB system. This is due to the dominating influence of the eluent costs because of the low solubility of the product. In general, higher solubilities will lead to an increasing influence of the adsorbent costs. For these cases, the productivity will become more important and, consequently, the SMB technique will become more advantageous in comparison with batch separation.

6. Nomenclature

A, B, C	parameters of the Van Deemter equation
c	liquid-phase concentration (g/cm^3)

c_p	liquid-phase concentration in the adsorbent pores (g/cm^3)
C_0	dimensionless liquid-phase concentration
C_{p0}	dimensionless particle concentration (g/cm^3)
C	costs (US$)
C^h	costs per hour (US$/h)
C^{spec}	specific costs (US$/g)
D_{ax}	axial dispersion (cm^2/s)
d_p	particle diameter (cm)
D_{pore}	pore diffusion coefficient (cm^2/s)
D_c	column diameter (cm)
Ec	specific eluent consumption (dm^3/g)
F	phase ratio
f_{ads}	specific adsorbent costs (US$/kg)
f_{feed}	specific feed costs (US$/g)
f_{el}	specific eluent costs (US$/dm^3)
HETP	height equivalent to a theoretical plate (cm)
k'	relative retention
k_{eff}	overall mass transfer coefficient (cm/s)
k_{0i}	constants
k_{film}	film mass transfer coefficient (cm/s)
k_m	lumped mass transfer coefficient (dm^3/s)
L_c	column length (cm)
L_f	loading factor
m	mass (g)
m_j	dimensionless flow-rates in SMB zones I to IV
$\dot{m}$	mass flow (g/s)
n_{refill}	number of refills
$n_{write\text{-}off}$	number of years of depreciation (years)
N	number of stages
Pe	Pèclet number
Pr	specific productivity (g dm^{-3} h^{-1})
q_s	saturation capacity (g/cm^3)
$\dot{Q}_j$	internal flow-rates in SMB zones I to IV (cm^3/s)
Re_p	particle Reynolds number
St_{eff}	modified Stanton number
t	time (s)
t_{period}	switch time (s)
t_{oper}	operation time (h)
t_{oper}^{max}	maximum operation time per year (h/year)
u_{int}	interstitial velocity (cm/s)
V	volume (cm^3)
x	space increment (cm)
y	solid-phase concentration (g/cm^3)
Y	yield
Z	dimensionless length

Greek letters

Δp	pressure drop (bar)
ε	porosity
ε_p	particle porosity
ε_t	total porosity
η_{fl}	dynamic viscosity (g/cm^3)
ρ_{app}	apparent density of adsorbent (kg/dm^3)
Θ	dimensionless time
ψ	constant of pressure drop correlation
χ	mass fraction

Subscripts

+	(+)-enantiomer
−	(−)-enantiomer
I, II, III, IV	zone in SMB unit
A	component in extract or raffinate
ads	adsorbent
cap	capital
crudeloss	lost of crude
cycl	cycle
el	eluent
inj	injection
invest	investment
life	lifetime
oper	operation
prod	product
sep	separation
SC	batch (**s**inge **c**olumn) unit
SMB	SMB unit

Acknowledgements

The financial support of the German Ministry of Education and Research (Bundesministerium für Bildung und Forschung BMBF) under grant number 03D0062B0 is very gratefully acknowledged. The

authors also thank the Max-Buchner-Stiftung for financial support. We further acknowledge fruitful discussions with Klaus Wekenborg and Matthias Grüger and their valuable input to this work. Finally, we gratefully thank Michael Schulte (Merck KGaA, Darmstadt, Germany) for his valuable contributions and support for our work.

References

[1] H. Colin, in: G. Gantesos, P.E. Barker (Eds.), Preparative and Production Scale Chromatography, Marcel Dekker, New York, 1993, p. 11.
[2] A. Felinger, G. Guiochon, J. Chromatogr. A 796 (1998) 59.
[3] D.B. Broughton, C.G. Gerhold, US Pat. 2 985 589, 1961.
[4] D.M. Ruthven, C.B. Ching, Chem. Eng. Sci. 44 (1989) 1011.
[5] G. Ganetsos, P.E. Barker, J.N. Ajongwen, in: G. Gantesos, P.E. Barker (Eds.), Preparative and Production Scale Chromatography, Marcel Dekker, New York, 1993, p. 375.
[6] R. Ditz, M. Schulte, J. Strube, Curr. Opin. Drug Discovery Dev. 1 (1998).
[7] A. Felinger, G. Guiochon, J. Chromatogr. 591 (1992) 31.
[8] A. Felinger, G. Guiochon, AIChE J. 40 (1994) 594.
[9] A. Felinger, G. Guiochon, J. Chromatogr. A 752 (1996) 31.
[10] G. Guiochon, S. Golshan Shirazi, A.M. Katti, Fundamentals of Preparative and Nonlinear Chromatography, Academic Press, Boston, MA, 1994.
[11] J. Strube, S. Haumreisser, H. Schmidt-Traub, M. Schulte, R. Ditz, Org. Proc. Res. Dev. A (1999).
[12] M. Morbidelli, M. Mazzotti, C. Migliorini, AIChE J. 46 (2000) 1384.
[13] G. Dünnebier, Ph.D. thesis, University of Dortmund, Dortmund, 2000.
[14] G. Storti, M. Mazotti, M. Morbidelli, S. Carra, AIChE J. 39 (1993) 471.
[15] B.B. Fish, R.W. Carr, R. Aris, AIChE J. 39 (1993) 1783.
[16] G. Zhong, G. Guiochon, Chem. Eng. Sci. 51 (1996) 4307.
[17] G. Dünnebier, K.-U. Klatt, Comp. Chem. Eng. Suppl. (1999) 195.
[18] A. Jupke, A. Epping, H. Schmidt-Traub, M. Schulte, in: Proceedings of SPICA 2000, Zürich, 2000.
[19] G. Dünnebier, A. Jupke, K.-U. Klatt, Chem.-Ing.-Tech. 72 (2000) 589.
[20] A.M. Katti, P. Jagland, Anal. Mag. 26 (1998) 38.
[21] J. Strube, U. Altenhöner, M. Meurer, H. Schmidt-Traub, M. Schulte, J. Chromatogr. A 769 (1997) 328.
[22] A. Epping, A. Jupke, H. Schmidt-Traub, M. Schulte, Chem. Eng. Sci. (submitted for publication).
[23] A. Jupke, A. Epping, J. Fricke, H. Schmidt-Traub, M. Schulte, Chem.-Ing.-Tech. 72 (2000) 593.
[24] T. Gu, Mathematical Modelling and Scale Up of Liquid Chromatography, Springer, New York, 1993.
[25] E. Glueckauf, in: Metcalfe and Cooper (Eds.), Ion Exchange and its Applications, Society of Chemical Industry, London, UK, 1955, p. 34.
[26] J.J. Van Deemter, F.J. Zuiderweg, A. Klingenberg, Chem. Eng. Sci. 5 (1956) 271.
[27] L.R. Snyder, in: C. Horvath (Ed.), High Performance Liquid Chromatography — Advances and Perspectives, Vol. 1, Academic Press, New York, 1980, p. 207.
[28] M. Morbidelli, M. Mazotti, G. Storti, J. Chromatogr. A 769 (1997) 3.
[29] J. Strube, A. Jupke, A. Epping, H. Schmidt-Traub, M. Schulte, R.M. Devant, Chirality 11 (1999) 440.
[30] G. Biressi, O. Ludemann-Homburger, M. Mazzotti, R.-M. Nicoud, M. Morbidelli, J. Chromatogr. A 876 (2000) 3.
[31] M. Schulte, R. Ditz, R.M. Devant, J.N. Kinkel, F. Charton, J. Chromatogr. A 769 (1997) 93.
[32] F. Charton, R.-M. Nicoud, J. Chromatogr. A 702 (1995) 97.
[33] B. Pynnonen, J. Chromatogr. A 827 (1998) 143.
[34] M. Schulte, J. Strube, J. Chromatogr. A 906 (2001) 399.
[35] O. Ludemann-Hombourger, M. Bailly, R.-M. Nicoud, Sep. Sci. Technol. 35 (2000) 1285.